

A Bayes–Sard Cubature Method

Toni Karvonen¹, Chris J. Oates^{2,3} and Simo Särkkä¹

¹Department of Electrical Engineering and Automation, Aalto University, Finland.

²School of Mathematics, Statistics and Physics, Newcastle University, UK.

³Alan Turing Institute, London, UK.

April 9, 2018

Abstract

This paper focusses on the formulation of numerical integration as an inferential task. To date, research effort has focussed on the development of *Bayesian cubature*, whose distributional output provides uncertainty quantification for the integral. However, the natural point estimators associated with Bayesian cubature do not, in general, correspond to standard cubature rules (e.g. Gaussian, Smolyak, quasi-Monte Carlo), which are widely-used and better-studied. To address this drawback, we present *Bayes–Sard cubature*, a general framework in which any cubature rule can be endowed with a meaningful probabilistic output. This is achieved by considering a Gaussian process model for the integrand, whose mean is a parametric regression model with an improper flat prior on each regression coefficient. The features in the regression model consist of test functions which are exactly integrated, with the remainder of the computational budget afforded to the non-parametric part in a manner similar to Sard. It is demonstrated that, through a judicious choice of test functions, any cubature rule can be recovered as the posterior mean in the Bayes–Sard output. The asymptotic convergence of the Bayes–Sard cubature method is established and our theoretical results are numerically verified.

1 Introduction

This paper considers the numerical approximation of an integral

$$\int_D f^\dagger d\nu \tag{1}$$

for some domain $D \subseteq \mathbb{R}^d$ and some (deterministic) integrand $f^\dagger : D \rightarrow \mathbb{R}$, where ν is a Borel probability measure on D . The approximation of Eqn. 1 is a fundamental task in applied mathematics and an important challenge for numerical computation in general. Indeed, the scope and ambition of modern scientific and industrial computer codes is such that the

integrand f^\dagger can often represent the output of a complex model. In such cases the evaluation of the integrand is associated with a substantial resource cost and, as a consequence, the total number of evaluations will be limited. The research challenge, in these circumstances, manifests not merely in the design of a cubature method but also in the assessment of the error associated to the method.

The *Bayesian cubature* (or, if $d = 1$, *quadrature*) method [Larkin, 1972; Diaconis, 1988; O’Hagan, 1991; Minka, 2000] combines a constructive approach to integration (i.e., based on an explicit approximation to the integrand) and a statistical approach to error assessment. In brief, let Ω be a probability space and consider a hypothetical Bayesian agent who represents their epistemic uncertainties in the form of a stochastic process $f: D \times \Omega \rightarrow \mathbb{R}$. This stochastic process must arise from a Bayesian regression model and be consistent with obtained evaluations of the true integrand, typically provided on a discrete point set $\{x_i\}_{i=1}^n \subset D$; that is $f(x_i, \omega) = f^\dagger(x_i)$ for almost all $\omega \in \Omega$. The stochastic process acts as a stochastic model for the integrand f^\dagger and implies, in particular, a stochastic model

$$\omega \mapsto \int_D f(\cdot, \omega) d\nu \tag{2}$$

representing the agent’s epistemic uncertainty for the value of the integral in Eqn. 1.

The output of the Bayesian cubature method is the law of the random variable in Eqn. 2. The mean of this output provides a numerical approximation to the integral, whilst the standard deviation indicates the extent of the agent’s uncertainty regarding the integral. The properties of this probabilistic output have been explored in detail for the case of a Gaussian stochastic process: In certain situations the mean has been shown to coincide with a kernel-based integration method [for an overview of such methods, see Oettershagen, 2017] that is rate-optimal [Bach, 2017; Briol et al., 2017], robust to misspecification of the agent’s belief [Kanagawa et al., 2016, 2017] and efficiently computable [Karvonen and Särkkä, 2018a,b]. The non-Gaussian case was explored empirically in Osborne et al. [2012a]; Gunter et al. [2014] and Chai and Garnett [2018], with related extensions appearing in Osborne et al. [2012b] and Oates et al. [2017]. The Bayesian cubature method has also received attention in the literature on *probabilistic numerics*; see Diaconis [1988]; O’Hagan [1992]; Hennig et al. [2015] and Cockayne et al. [2017] for general background.

However, it remains the case that non-probabilistic numerical integration methods, such as Gaussian cubatures [Gautschi, 2004] and quasi-Monte Carlo methods [Hickernell, 1998], are often preferred, due in part to how their ease-of-use or reliability are perceived. It has been long known the trapezoidal rule and other higher-order spline methods [Davis and Rabinowitz, 2007] can be naturally cast as Bayesian cubatures if the stochastic process f is selected suitably [Diaconis, 1988], but there are few such results for other methods. In the realm of numerical solvers for differential equations, some special cases have been explored by Schober et al. [2014] and Teymur et al. [2016], and even though Särkkä et al. [2016] and Karvonen and Särkkä [2017] have pointed out that there is in fact a close connection between Gaussian cubature methods and kernel-based methods, in the sense that Gaussian cubature can be viewed as a special (in fact, degenerate) case of a kernel method, no satisfactory and flexible overall framework has been developed.

This paper argues that the perceived performance gap between probabilistic and non-probabilistic methods should be reconsidered. In particular, it is demonstrated that *any* cubature rule, no matter how constructed, can be cast as a (generalised) Bayesian cubature rule and endowed with a meaningful, non-degenerate probabilistic output. Our specific contributions are detailed next.

1.1 Our Contribution

The contribution of this work is two-fold:

- First, we consider a non-parametric Bayesian regression model augmented with a parametric component. In the numerical integration context, this regression model is the basis of a *generalised Bayesian cubature* method that is contained in Thm. 3.13. The features in the parametric component, that is the pre-specified finite set of basis functions, will be denoted π . Then, an improper uniform prior limit on the regression coefficients [O’Hagan, 1978; Rasmussen and Williams, 2006, Sec. 2.7] is studied. In the numerical integration context, again, this regression model is the basis of the *Bayes–Sard cubature* method. It is demonstrated that the mean of the Bayes–Sard output takes the form of a cubature rule for which functions in π are exactly integrated. This is reminiscent of the method of Sard [1949] for selecting the “best” quadrature weights for given n nodes by fixing a polynomial space of degree $m < n$ on which the quadrature rule must be exact and disposing of the remaining $n - 1 - m$ degrees of freedom by minimising an appropriate error functional. See also Schoenberg [1964] and Larkin [1970]. This connection is most clearly seen in Rmk. 3.19. The main result is Thm. 3.16, which presents expressions for the mean and variance of the Bayes–Sard output.

The estimator provided by the mean of the Bayes–Sard output has appeared before in non-probabilistic contexts, though it does not seem to have been widely used. Indeed, we show that this cubature rule is closely related to interpolation with conditionally positive definite kernels [Wendland, 2005, Chapter 8]; a special case of which appeared in Bezhaev [1991]. An equivalent version was also recently proposed in DeVore et al. [2017, Section 5.2] in the context of optimal approximation in reproducing kernel Hilbert spaces.

- Second, when the dimension of the function space π matches the number of cubature nodes, it is demonstrated that the improper uniform limit can be used to recover any cubature rule as the mean of the Bayes–Sard output. Or, more succinctly, “all cubature rules have probabilistic counterparts”. More importantly, the variance of the associated probability distribution is non-trivial, computable, and can be related to the classical worst-case error in a particular reproducing kernel Hilbert space, through a mechanism that is well-studied. In the terminology of Bayesian decision theory [Berger, 2013], the Bayes–Sard framework thus demonstrates that “any cubature rule is a Bayes decision rule for some prior”; a concrete instantiation of the *complete class* theorem

of Wald [1947]. As a consequence, it is possible to simultaneously achieve reliable performance due to, for example, polynomial exactness, *and* perform formal uncertainty quantification for the integral. These results appear in Sec. 3.2.4 as Thm. 3.20 and Cor. 3.21.

The remainder of the paper proceeds as follows. In Sec. 2 we introduce the notation and terminology that will be used. Sec. 3 contains the methodological development, first for general Gaussian process regression and then for cubature. Sec. 3.1.3 also reviews the concept of unisolvent sets, necessary for non-singularity of improper limits that we consider. The proposed Bayes–Sard method is empirically assessed in Sec. 4 using three numerical examples. Last, some conclusions are drawn in Sec. 5.

2 Preliminaries

This section introduces the notation and terminology that will be used.

Domain: For $d \in \mathbb{N}$, let D be a domain in \mathbb{R}^d . If bounded, let ∂D denote the boundary of D . A bounded domain D is said to satisfy an *interior cone condition* if there exists an angle $\theta \in (0, \frac{\pi}{2})$ and a radius $r > 0$ such that for each $x \in D$ a unit vector $\xi(x)$ exists such that the cone $\{x + \lambda y : y \in \mathbb{R}^d, \|y\|_2 = 1, y^\top \xi(x) \geq \cos \theta, \lambda \in [0, r]\}$ is contained in D .

Integrand: Let $C^r(D)$ denote the set of r -times continuously differentiable functions on a domain D , equipped with the supremum norm. In this paper it will be assumed that $f^\dagger \in C^0(D)$. A consequence of this assumption is that point evaluation, that is $f^\dagger(x)$, is well-defined for all $x \in D$.

Cubature: Let $I : C^0(D) \rightarrow \mathbb{R}$ denote the integration operator $I(f) = \int_D f d\nu$. A generic *cubature rule* based on n points is defined to be a mapping $I_n : C^0(D) \rightarrow \mathbb{R}$ of the form

$$I_n(f) = \sum_{i=1}^n w_i f(x_i)$$

for some *weights* $w_i \in \mathbb{R}$ and points (or *nodes*) $x_i \in D$. In the special case where $w_i = \frac{1}{n}$ we say that the cubature rule is *uniformly* weighted. A cubature rule I_n is said to be *exact* on a set $\pi \subset C^0(D)$ if it holds that $I_n(p) = I(p)$ for all $p \in \pi$.

Function Spaces: Throughout this paper we work with a finite-dimensional linear subspace π of real-valued functions defined on $D \subseteq \mathbb{R}^d$. No regularity conditions are imposed on functions in π . The dimension of π is $Q := \dim(\pi)$ and a basis for it is denoted $\{p_1, \dots, p_Q\}$. The space that we most often use is $\Pi_m(\mathbb{R}^d)$, the space of d -variate polynomials of degree at most m :

$$\Pi_m(\mathbb{R}^d) := \text{span}\{x^\alpha : |\alpha| \leq m\}$$

where $\alpha \in \mathbb{N}_0^d$ is a multi-index, $x^\alpha = x_1^{\alpha_1} \cdots x_d^{\alpha_d}$ and $|\alpha| = \alpha_1 + \cdots + \alpha_d$. The dimension of this space is

$$\dim(\Pi_m(\mathbb{R}^d)) = \binom{m+d}{d}.$$

Let also

$$H^\alpha(D) := \{f \in L^2(D) : D^\beta f \in L^2(D) \text{ for every } |\beta| \leq \alpha\}$$

denote a standard Sobolev space, where $D^\beta f$ is to be interpreted as a weak derivative $\partial_{x_1}^{\beta_1} \cdots \partial_{x_d}^{\beta_d} f$ with β a multi-index, equipped with the inner product

$$\langle f, g \rangle_{H^\alpha(D)} = \sum_{|\beta| \leq \alpha} \langle D^\beta f, D^\beta g \rangle_{L^2(D)}.$$

Kernels and Reproducing Kernel Hilbert Spaces: To a bivariate function $k : D \times D \rightarrow \mathbb{R}$ which is (a) symmetric (i.e. $k(x, y) = k(y, x)$ for all $x, y \in D$) and (b) positive definite (i.e. $\sum_{i,j=1}^n \alpha_i \alpha_j k(x_i, x_j) \geq 0$ for all $n \in \mathbb{N}$, $\alpha_i \in \mathbb{R}$ and $x_i \in D$) we associate a *reproducing kernel Hilbert space* (RKHS) $H(k)$ of functions on D , equipped with canonical inner product and norm respectively denoted $\langle \cdot, \cdot \rangle_k$ and $\|\cdot\|_k$. The *reproducing property* states that $\langle h, k(\cdot, x) \rangle_k = h(x)$ for all $h \in H(k)$ and $x \in D$ and such a k as described will be called a *kernel* in this work. See Berlinet and Thomas-Agnan [2011] for the relevant background.

Convergence: For sequences $(a_n)_{n \in \mathbb{N}}$ and $(b_n)_{n \in \mathbb{N}}$, we write $a_n \lesssim b_n$ if the ratio a_n/b_n is bounded above for sufficiently large $n \in \mathbb{N}$.

3 Methods

This section contains our novel methodological development. The focus is on constructive integration methods and, as such, we must first posit a statistical model for the integrand. To this end, in Section 3.1 we recall the Gaussian process regression framework and its specialisation to the case of an improper flat prior on the mean functional. We also establish when this limit is well-defined. Next, Section 3.2 exploits the Gaussian process machinery in order to construct the Bayes–Sard cubature method itself. Finally, in Section 3.3 some of the main theoretical properties of the Bayes–Sard method are rigorously established.

3.1 A Gaussian Process Regression Model

The purpose of this section is to set up a Gaussian process regression framework. Our first task, in Section 3.1.1, is to recall the standard Gaussian process prior model, and in Section 3.1.2, the Gaussian process posterior in a regression context. Then a technical detail, unisolvency, is discussed in Section 3.1.3. Last, in Section 3.1.4, we present our proposed prior model as an improper prior limit and establish when this limit is well-defined.

Most of the developments of this section have appeared in O’Hagan [1978]; see also [Rasmussen and Williams, 2006, Section 2.7]. In particular, our main result, Thm. 3.9, is essentially Thm. 2 of O’Hagan [1978]. Nevertheless, we find it instructive to present all the derivations in full.

3.1.1 Gaussian Process Prior

Recall that a *Gaussian process* is a function-valued random variable $\omega \mapsto f(\cdot, \omega)$ such that $f(\cdot, \omega) \in C^0(D)$ and $\omega \mapsto Lf(\cdot, \omega)$ is a (univariate) Gaussian for all continuous linear functionals L on $C^0(D)$. Here ω denotes a generic element of an underlying probability space Ω . See Bogachev [1998] for further background. Following the notational convention of Rasmussen and Williams [2006], we suppress the argument ω and denote by $f(x) \sim \mathcal{GP}(s(x), k(x, x'))$ a Gaussian process with mean function $s \in C^0(D)$ and covariance function $k \in C^0(D \times D)$, where k is a kernel. The characterising property of this Gaussian process is that

$$\begin{bmatrix} f(x_1) \\ \vdots \\ f(x_n) \end{bmatrix} \sim \mathcal{N} \left(\begin{bmatrix} s(x_1) \\ \vdots \\ s(x_n) \end{bmatrix}, \begin{bmatrix} k(x_1, x_1) & \dots & k(x_1, x_n) \\ \vdots & \ddots & \vdots \\ k(x_n, x_1) & \dots & k(x_n, x_n) \end{bmatrix} \right)$$

for all sets $X = \{x_1, \dots, x_n\} \subset D$.

Our starting point in this paper will be to endow a hypothetical Bayesian agent with the following prior model for the integrand:

Definition 3.1 (Prior). Let π denote a finite-dimensional linear subspace of real-valued functions on D and $\{p_1, \dots, p_Q\}$ a basis of π , so that $Q = \dim(\pi)$. Then we consider the following hierarchical *prior* model:

$$\begin{aligned} f(x) \mid \gamma &\sim \mathcal{GP}(s(x), k(x, x')), \\ s(x) \mid \gamma &= \sum_{j=1}^Q \gamma_j p_j(x), \\ \gamma &\sim \mathcal{N}(\eta, \Sigma) \end{aligned}$$

for some mean $\eta \in \mathbb{R}^Q$ and a positive-definite covariance matrix $\Sigma \in \mathbb{R}^{Q \times Q}$.

The mean function $s \in \pi$ is parametrised by $\gamma_1, \dots, \gamma_Q \in \mathbb{R}$. Such a prior could arise, for example, when a parametric linear regression model is assumed and a non-parametric discrepancy term added to allow for mis-specification of the parametric part [Kennedy and O’Hagan, 2001]. The prior enjoys some similarities to universal kriging models; see for example Ba and Joseph [2012].

3.1.2 Gaussian Process Posterior

In a regression context, the data consist of input-output pairs $\mathcal{D}_X = \{(x_i, f^\dagger(x_i))\}_{i=1}^n$ based on a finite point set $X = \{x_1, \dots, x_n\} \subset D$. This paper does not consider adaptive cubature

methods – focussing instead on uncertainty quantification – and therefore the point set is considered fixed. Our interest, in this section, is in the Bayesian agent’s posterior distribution for the integrand, after the data \mathcal{D}_X are observed. Let f_X (resp. f_X^\dagger) be the column vector with entries $f(x_i)$ (resp. $f^\dagger(x_i)$).

The *posterior* is defined as the law of the stochastic process, denoted $f \mid \mathcal{D}_X$, which is obtained when the original stochastic process $\omega \mapsto f(\cdot, \omega)$ is restricted to the set $\{\omega \in \Omega : f_X = f_X^\dagger\}$. Though it is somewhat technical to make formal, it is well-known that the posterior is again a Gaussian stochastic process [technical details can be found in, e.g., Owhadi and Scovel, 2015]. Indeed: Let $p(x)$ be the row vector with entries $p_j(x)$ and let P_X denote the $n \times Q$ *Vandermonde matrix* with $[P_X]_{i,j} = p_j(x_i)$. Let $k_X(x)$ denote the row vector with entries $k(x, x_j)$ and let K_X denote the *kernel matrix* with $[K_X]_{i,j} = k(x_i, x_j)$.

Theorem 3.2 (Posterior). *Under the prior in Def. 3.1, we have that*

$$f(x) \mid \mathcal{D}_X \sim \mathcal{GP}(s_{X,\Sigma}(f^\dagger)(x), k_{X,\Sigma}(x, x'))$$

where

$$s_{X,\Sigma}(f^\dagger)(x) = k_X(x)\alpha + p(x)\beta, \tag{3}$$

$$k_{X,\Sigma}(x, x') = k(x, x') + p(x)\Sigma p(x')^\top - [k_X(x) + p(x)\Sigma P_X^\top][K_X + P_X\Sigma P_X^\top]^{-1}[k_X(x') + p(x')\Sigma P_X^\top]^\top \tag{4}$$

and the coefficients α and β are defined via the invertible linear system

$$\begin{bmatrix} K_X & P_X \\ P_X^\top & -\Sigma^{-1} \end{bmatrix} \begin{bmatrix} \alpha \\ \beta \end{bmatrix} = \begin{bmatrix} f_X^\dagger \\ -\eta \end{bmatrix}. \tag{5}$$

Proof. Under the hierarchical prior we have the marginal

$$f(x) \sim \mathcal{GP}(p(x)\eta, k(x, x') + p(x)\Sigma p(x')^\top).$$

Thus standard formulae for the conditioning of a Gaussian process [Eqns. 2.25, 2.26 in Rasmussen and Williams, 2006] can be used:

$$s_{X,\Sigma}(f^\dagger)(x) = p(x)\eta + [k_X(x) + p(x)\Sigma P_X^\top][K_X + P_X\Sigma P_X^\top]^{-1}[f_X^\dagger - P_X\eta], \tag{6}$$

$$k_{X,\Sigma}(x, x') = k(x, x') + p(x)\Sigma p(x')^\top - [k_X(x) + p(x)\Sigma P_X^\top][K_X + P_X\Sigma P_X^\top]^{-1}[k_X(x') + p(x')\Sigma P_X^\top]^\top. \tag{7}$$

The coefficients α and β are therefore

$$\alpha = [K_X + P_X\Sigma P_X^\top]^{-1}[f_X^\dagger - P_X\eta], \tag{8}$$

$$\beta = \eta + \Sigma P_X^\top [K_X + P_X\Sigma P_X^\top]^{-1}[f_X^\dagger - P_X\eta]. \tag{9}$$

It can be verified by substitution that $P_X^\top\alpha - \Sigma^{-1}\beta = -\eta$ and the interpolation equations $K_X\alpha + P_X\beta = f_X^\dagger$ hold. This allows us to provide the equivalent characterisation of α and β

in terms of the linear system in Eqn. 5. To see that this linear system is invertible, we can use the block matrix determinant formula

$$\det \left(\begin{bmatrix} K_X & P_X \\ P_X^\top & -\Sigma^{-1} \end{bmatrix} \right) = \det(-\Sigma^{-1}) \det(K_X + P_X \Sigma P_X^\top).$$

That is, since Σ is a positive definite covariance matrix, the block matrix is invertible if and only if $K_X + P_X \Sigma P_X^\top$ is invertible. This is indeed true because, for instance, $K_X + P_X \Sigma P_X^\top$ is the covariance matrix for the random vector f_X under the prior, which is well-defined. \square

Note that the posterior is consistent with the data \mathcal{D}_X , in the sense that the posterior mean $s_{X,\Sigma}(f^\dagger)(x)$ coincides with the value $f^\dagger(x)$ at the locations $x \in X$ and, moreover, the posterior variance vanishes at each $x \in X$. These two facts imply that sample paths from $f \mid \mathcal{D}_X$ almost surely satisfy $f_X = f_X^\dagger$. Note also that the posterior covariance function depends on X and Σ but not on the values of the integrand nor on the mean η of the parametric part of the prior.

Remark 3.3 (Bayesian cubature). Based on Eqns. 6 and 7, it is apparent that if we set $\eta = 0$ and $\Sigma = 0$, then the posterior reduces to a Gaussian process with mean and covariance

$$\begin{aligned} s_{X,0}(f^\dagger)(x) &= k_X(x) K_X^{-1} f_X^\dagger, \\ k_{X,0}(x, x') &= k(x, x') - k_X(x) K_X^{-1} k_X(x')^\top. \end{aligned}$$

These equations characterise the stochastic process used in the conventional Bayesian cubature method [Minka, 2000; Briol et al., 2017].

The following Lagrange form [Wendland, 2005, Section 11.1] of the posterior will be useful:

Theorem 3.4 (Lagrange form for the posterior). *The posterior mean and covariance functions in Eqns. 3 and 4 can be written in the Lagrange form*

$$\begin{aligned} s_{X,\Sigma}(f^\dagger)(x) &= u_{X,\Sigma}(x)^\top f_X^\dagger - v_{X,\Sigma}(x)^\top \eta, \\ k_{X,\Sigma}(x, x') &= k(x, x') + p(x) \Sigma p(x')^\top - [k_X(x) + p(x) \Sigma P_X^\top] u_{X,\Sigma}(x'), \end{aligned} \quad (10)$$

where

$$u_{X,\Sigma}(x) := [K_X + P_X \Sigma P_X^\top]^{-1} [k_X(x) + p(x) \Sigma P_X^\top]^\top \quad (11)$$

is a vector of Lagrange cardinal functions and $v_{X,\Sigma}(x) := \Sigma [P_X^\top u_{X,\Sigma}(x) - p(x)^\top]$. These functions are obtained from the invertible linear system

$$\begin{bmatrix} K_X & P_X \\ P_X^\top & -\Sigma^{-1} \end{bmatrix} \begin{bmatrix} u_{X,\Sigma}(x) \\ v_{X,\Sigma}(x) \end{bmatrix} = \begin{bmatrix} k_X(x)^\top \\ p(x)^\top \end{bmatrix} \quad (12)$$

and satisfy the cardinality property $[u_{X,\Sigma}(x_j)]_i = \delta_{ij}$ and $[v_{X,\Sigma}(x_j)]_i = 0$ for every $i, j \in \{1, \dots, n\}$.

Proof. From Eqns. 3 and 5, the posterior mean is

$$s_{X,\Sigma}(f^\dagger)(x) = \begin{bmatrix} k_X(x) & p(x) \end{bmatrix} \begin{bmatrix} \alpha \\ \beta \end{bmatrix} = \begin{bmatrix} k_X(x) & p(x) \end{bmatrix} \begin{bmatrix} K_X & P_X \\ P_X^\top & -\Sigma^{-1} \end{bmatrix}^{-1} \begin{bmatrix} f_X^\dagger \\ -\eta \end{bmatrix},$$

and this can be written as $s_{X,\Sigma}(f^\dagger)(x) = u_{X,\Sigma}(x)^\top f_X^\dagger - v_{X,\Sigma}(x)^\top \eta$ where $u_{X,\Sigma}(x)$ and $v_{X,\Sigma}(x)$ are obtained from the linear system in Eqn. 12. The expression for the posterior covariance follows by inserting $u_{X,\Sigma}(x')$, as given in Eqn. 11, into Eqn. 4. The cardinality property follows after we recognise that, setting $x = x_j$, Eqn. 12 is solved by $u_{X,\Sigma}(x_j) = e_j$ (the j th unit coordinate vector) and $v_{X,\Sigma}(x_j) = 0$. \square

The need for the Bayesian agent to elicit a covariance matrix Σ appears to prevent this prior model from being automatically used. For this reason, in the subsequent sections we consider the *flat prior limit* as $\Sigma^{-1} \rightarrow 0$, which corresponds to a particular encoding of an absence of prior information about the value of the parameter γ in Def. 3.1. However, it must first be established that Eqns. 5 and 12 are not singular in this limit. For this reason, we need the notion of a unisolvent point set, introduced next.

3.1.3 Unisolvent Point Sets

This section briefly recalls the concept of a unisolvent point set; see Wendland [2005, Chapter 8] or Fasshauer [2007, Chapters 6] for a more detailed account¹.

Definition 3.5 (Unisolvency). Let π denote a finite-dimensional linear subspace of real-valued functions on D . A point set $X = \{x_1, \dots, x_n\} \subset D$ with $n \geq \dim(\pi)$ is called π -*unisolvent* if the zero functional is the only element in π that vanishes on X .

The following proposition provides an equivalent operational characterisation of unisolvency:

Proposition 3.6. Let $\{p_1, \dots, p_Q\}$ denote a basis of π , so that $Q = \dim(\pi)$. Then a point set X is π -unisolvent if and only if the $n \times Q$ Vandermonde matrix P_X is of full rank.

Example 3.7 (Cartesian product of a unisolvent set). As a simple example of how one can generate a unisolvent set in \mathbb{R}^d , consider the Cartesian grid $X = Z^d$ for a $\Pi_{m-1}(\mathbb{R})$ -unisolvent set $Z = \{z_1, \dots, z_m\} \subset \mathbb{R}$ (i.e., the points z_i are distinct). Then for any d -variate polynomial

$$p \in \Pi := \text{span}\{x^\alpha : \alpha \leq m - 1\},$$

the univariate polynomial

$$p_j(z) = p(z_{\alpha_1}, \dots, z_{\alpha_{j-1}}, z, z_{\alpha_{j+1}}, \dots, z_{\alpha_d})$$

is of degree at most $m - 1$ and, for any indices $j \in \{1, \dots, d\}$ and $\alpha_1, \dots, \alpha_d \in \{1, \dots, m - 1\}$, the polynomial p_j cannot vanish on Z unless it is the zero polynomial. It follows that p cannot vanish on X unless $p \equiv 0$. Therefore X is Π -unisolvent. Note that $\#X = \dim(\Pi) = m^d$.

¹Note that we work with a slightly more general definition of unisolvency than these authors, not constraining ourselves to polynomial spaces.

Example 3.8 (Not all sets are unisolvent). As a counterexample, consider six points $X = \{(x_i, y_i), i = 1, \dots, 6\}$ on a unit circle in \mathbb{R}^2 . These points are not $\Pi_2(\mathbb{R}^d)$ -unisolvent: the associated Vandermonde matrix

$$P_X = \begin{bmatrix} 1 & x_1 & y_1 & x_1 y_1 & x_1^2 & y_1^2 \\ 1 & x_2 & y_2 & x_2 y_2 & x_2^2 & y_2^2 \\ 1 & x_3 & y_3 & x_3 y_3 & x_3^2 & y_3^2 \\ 1 & x_4 & y_4 & x_4 y_4 & x_4^2 & y_4^2 \\ 1 & x_5 & y_5 & x_5 y_5 & x_5^2 & y_5^2 \\ 1 & x_6 & y_6 & x_6 y_6 & x_6^2 & y_6^2 \end{bmatrix}$$

for the canonical polynomial basis is not of full rank as the first column is the sum of the last two columns.

Intuitively, “almost all” point sets are unisolvent, but to actually verify that an arbitrary point set X is unisolvent, from Proposition 3.6 it is required to compute the rank of the Vandermonde matrix P_X , which entails a super-linear computational cost [Sauer and Xu, 1995]. However, certain point sets are guaranteed to be unisolvent:

- When π is a Chebyshev system (so that its basis functions are so-called *generalised polynomials*) in one dimension, any set $X \subset \mathbb{R}$ of distinct points is π -unisolvent [Karlin and Studden, 1966].
- For π spanned by the indicator functions $\mathbb{1}_{A_1}, \dots, \mathbb{1}_{A_n}$ of disjoint sets $A_i \subset D$ such that $x_i \in A_i$, the set X is π -unisolvent and P_X is the $n \times n$ identity matrix.
- *Padua points* on $[-1, 1]^2$ are known to be unisolvent with respect to polynomial spaces [Caliari et al., 2005].
- Recent algorithms for generating moderate number of points for polynomial interpolation, with a unisolvency guarantee on the output, can be used [Sauer and Xu, 1995; Gunzburger and Teckentrup, 2014].

Henceforth we restrict attention to point sets X which are π -unisolvent.

3.1.4 Flat Prior Limit

The focus now returns to the flat prior limit. In this section we ask whether the Gaussian process posterior is well-defined in this limit. It turns out that the answer is positive, provided that the point set is unisolvent:

Theorem 3.9 (Flat prior limit). *Assume that X is a π -unisolvent set. For the prior in Def. 3.1, and in the limit $\Sigma^{-1} \rightarrow 0$, we have that $s_{X, \Sigma}(f^\dagger) \rightarrow s_X(f^\dagger)$ and $k_{X, \Sigma} \rightarrow k_X$ pointwise, where*

$$s_X(f^\dagger)(x) = k_X(x)\alpha + p_X(x)\beta, \tag{13}$$

$$k_X(x, x') = k(x, x') - k_X(x)K_X^{-1}k_X(x')^\top + [k_X(x)K_X^{-1}P_X - p(x)][P_X^\top K_X^{-1}P_X]^{-1}[k_X(x')K_X^{-1}P_X - p(x')]^\top, \tag{14}$$

and the coefficients α and β are defined from the invertible linear system implied by the equations

$$\begin{bmatrix} K_X & P_X \\ P_X^\top & 0 \end{bmatrix} \begin{bmatrix} \alpha \\ \beta \end{bmatrix} = \begin{bmatrix} f_X^\dagger \\ -\eta \end{bmatrix}. \quad (15)$$

Proof. For the mean function, the limit can just be taken in the linear system of Eqn. 5 and it is required is to verify that this system can be inverted. From an application of the formula for a block matrix determinant we have that the determinant of the matrix in Eqn. 15 equals $\det(-P_X^\top K_X^{-1} P_X) \det(K_X)$, where $\det(K_X) > 0$. Because X is π -unisolvent, P_X is of full rank and consequently the matrix $P_X^\top K_X^{-1} P_X$ is invertible. That is, the block matrix is invertible.

The covariance function requires more work. To this end, the Woodbury matrix identity yields

$$[K_X + P_X \Sigma P_X^\top]^{-1} = K_X^{-1} - K_X^{-1} P_X [\Sigma^{-1} + P_X^\top K_X^{-1} P_X]^{-1} P_X^\top K_X^{-1}.$$

Denoting $L_X := P_X^\top K_X^{-1} P_X$ and inserting the above into Eqn. 7 produces

$$\begin{aligned} k_{X,\Sigma}(x, x') &= k(x, x') - k_X(x) K_X^{-1} k_X(x')^\top + p(x) \Sigma p(x')^\top - p(x) \Sigma L_X \Sigma p(x')^\top \\ &\quad - k_X(x) K_X^{-1} P_X \Sigma p(x')^\top - p(x) \Sigma P_X^\top K_X^{-1} k_X(x')^\top \\ &\quad + k_X(x) K_X^{-1} P_X [\Sigma^{-1} + L_X]^{-1} P_X^\top K_X^{-1} k_X(x')^\top \\ &\quad + k_X(x) K_X^{-1} P_X [\Sigma^{-1} + L_X]^{-1} L_X \Sigma p(x')^\top \\ &\quad + p(x) \Sigma L_X [\Sigma^{-1} + L_X]^{-1} P_X^\top K_X^{-1} k_X(x')^\top \\ &\quad + p(x) \Sigma L_X [\Sigma^{-1} + L_X]^{-1} L_X \Sigma p(x')^\top. \end{aligned} \quad (16)$$

For small enough Σ^{-1} we can write the Neumann series

$$[\Sigma^{-1} + L_X]^{-1} = L_X^{-1} [I - (L_X \Sigma)^{-1} + (L_X \Sigma)^{-2} - \dots].$$

Therefore we have the trio of results

$$\begin{aligned} K_X^{-1} P_X [\Sigma^{-1} + L_X]^{-1} P_X^\top K_X^{-1} &= K_X^{-1} P_X L_X^{-1} P_X^\top K_X^{-1} + \mathcal{O}(\Sigma^{-1}), \\ K_X^{-1} P_X [\Sigma^{-1} + L_X]^{-1} L_X \Sigma &= K_X^{-1} P_X \Sigma - K_X^{-1} P_X L_X^{-1} + \mathcal{O}(\Sigma^{-1}), \\ \Sigma L_X [\Sigma^{-1} + L_X]^{-1} L_X \Sigma &= \Sigma L_X \Sigma - \Sigma + L_X^{-1} + \mathcal{O}(\Sigma^{-1}). \end{aligned}$$

Inserting these into Eqn. 16 yields, after some cancellations and taking the limit $\Sigma^{-1} \rightarrow 0$,

$$\begin{aligned} k_X(x, x') &= k(x, x') - k_X(x) K_X^{-1} k_X(x')^\top \\ &\quad + [k_X(x) K_X^{-1} P_X - p(x)] [P_X^\top K_X^{-1} P_X]^{-1} [k_X(x') K_X^{-1} P_X - p(x')]^\top, \end{aligned}$$

as claimed. \square

The flat prior limit of the posterior also admits a Lagrange representation:

Theorem 3.10 (Lagrange form in the flat prior limit). *Assume that X is a π -unisolvent set. The posterior mean and covariance in Eqns. 13 and 14 can be written as*

$$\begin{aligned} s_X(f^\dagger)(x) &= u_X(x)f_X^\dagger - v_X(x)\eta, \\ k_X(x, x') &= k(x, x') - k_X(x)K_X^{-1}k_X(x')^\top + [k_X(x)K_X^{-1}P_X - p(x)]v_X(x') \end{aligned} \quad (17)$$

where

$$\begin{aligned} v_X(x) &:= [P_X^\top K_X^{-1}P_X]^{-1}[k_X(x)K_X^{-1}P_X - p(x)]^\top, \\ u_X(x) &:= K_X^{-1}[k_X(x)^\top - P_X v_X(x)]^\top \end{aligned}$$

are obtained from the solution of the invertible linear system

$$\begin{bmatrix} K_X & P_X \\ P_X^\top & 0 \end{bmatrix} \begin{bmatrix} u_X(x) \\ v_X(x) \end{bmatrix} = \begin{bmatrix} k_X(x)^\top \\ p(x)^\top \end{bmatrix}$$

and have the cardinality properties $[u_X(x_j)]_i = \delta_{ij}$ and $[v_X(x_j)]_i = 0$ for every $i, j \in \{1, \dots, n\}$.

The proof is similar to that of Thm. 3.4 and is therefore omitted. Note the reversal in the roles of $u_{X, \Sigma}$ and v_X in Eqns. 10 and 17 for the posterior covariance. The following observation will be important:

Proposition 3.11 (Elements of π are reproduced). *Assume that X is a π -unisolvent set and that $\{p_1, \dots, p_Q\}$ form a basis for π . If $\eta = 0$, then $s_X(p) = p$ whenever $p \in \pi$.*

Proof. If $p \in \pi$, there exist coefficients $\beta'_1, \dots, \beta'_Q$ such that $p = \sum_{i=1}^Q \beta'_i p_i$. That is, a particular solution of Eqn. 15 is $\alpha = 0$ and $\beta = \beta'$. The linear system being invertible, this must be the only solution. We deduce that $s_X(p) = p$. \square

In particular, if $\dim(\pi) = n$, it is easy to see that the posterior mean reduces to the unique interpolant in π to the data \mathcal{D}_X while the posterior covariance is non-zero. This observation will form the basis of endowing any cubature rule with a non-degenerate probabilistic output in Sec. 3.2.4.

Note that a different limiting process can be used to obtain a posterior mean that is a polynomial interpolant. Namely, consider conventional Gaussian process regression (i.e., $\eta = 0$ and $\Sigma = 0$; recall Rmk. 3.3) with an infinitely smooth isotropic kernel having length-scale ℓ . Then it has been shown that the posterior mean converges to a polynomial interpolant to the data as $\ell \rightarrow \infty$ [Driscoll and Fornberg, 2002; Schaback, 2005; Lee et al., 2007]. However, such a construction is of little interest to us because the associated posterior covariance vanishes, such that uncertainty is not being quantified.

Remark 3.12 (An equivalent kernel perspective). There is a well-understood equivalence between Gaussian process regression and optimal interpolation in reproducing kernel Hilbert spaces: Let $\{p_1, \dots, p_Q\}$ be a basis for π and define the kernel $k_\pi(x, x') = \sum_{i=1}^Q p_i(x)p_i(x')$. Consider the kernel

$$k_\sigma(x, x') = k(x, x') + \sigma^2 k_\pi(x, x')$$

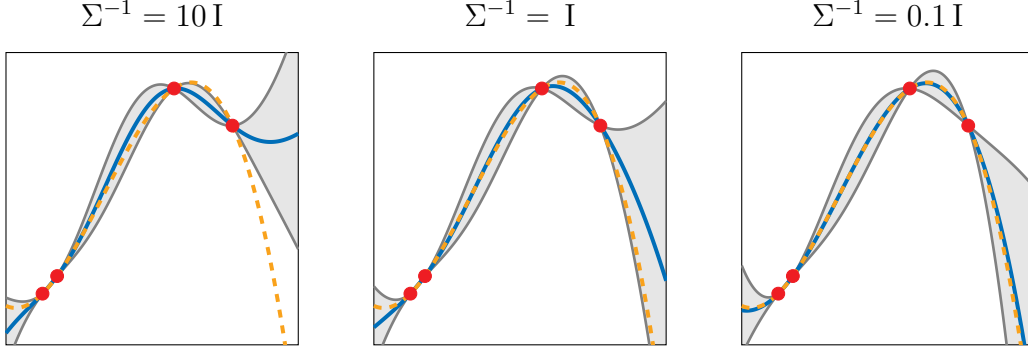


Figure 1: Posterior mean (blue) and 95% credible intervals (gray) given four data points (red) for the prior model of Def. 3.1 with $\eta = 0$ and $\pi = \Pi_3(\mathbb{R})$. The kernel was the Gaussian kernel (25) with length-scale $\ell = 0.8$. The unique polynomial interpolant of degree 3 to the data (dashed) is plotted for comparison. Note convergence of the posterior mean to the polynomial interpolant as $\Sigma^{-1} \rightarrow 0$.

for $\sigma > 0$. Then the reproducing kernel Hilbert space induced by k_σ corresponds to the set

$$H(k_\sigma) = \{f + p : f \in H(k), p \in \pi\}$$

equipped with a particular σ -dependent inner product. It can be shown that the interpolant with minimal norm in $H(k_\sigma)$ is unique and given by

$$s_{X,\sigma}(f^\dagger)(x) = [k_X(x) + \sigma^2 k_{\pi,X}(x)][K_X + \sigma^2 P_X P_X^\top]^{-1} f_X^\dagger,$$

where the row vector $k_{\pi,X}(x)$ has the elements $k_\pi(x, x_j)$. When $\eta = 0$, it is straightforward to show that $s_{X,\sigma}(f^\dagger) = s_{X,\Sigma}(f^\dagger)$ for $\Sigma = \sigma^2 I$ and thus $s_{X,\sigma}(f^\dagger) \rightarrow s_X(f^\dagger)$ pointwise as $\sigma \rightarrow \infty$. The kernel interpolation operator s_X is well-studied and the reader is referred to, for example, Sec. 8.5 of Wendland [2005]. This connection will also be discussed further in Sec. 3.2.3.

This completes the construction of a regression model for the integrand. Fig. 1 depicts the associated posterior distribution with three different selections for Σ . Next we turn our attention to estimation of the unknown scalar value of the integral.

3.2 The Bayes–Sard Framework

In this section we introduce our Bayes–Sard cubature method. This is a generalisation of the standard Bayesian cubature method, based on the prior model with $\Sigma^{-1} \rightarrow 0$, studied in Sec. 3.1.4. After the method has been defined, we expose some of its important properties – including its connection to classical cubature rules – in Sec. 3.2.4.

3.2.1 A Generalisation of Bayesian Cubature

In Bayesian cubature, uncertainty quantification for the integral $I(f^\dagger)$ is conducted by modelling the integrand as a Gaussian process $f : D \times \Omega \rightarrow \mathbb{R}$. The output of Bayesian cubature is the push-forward $\omega \mapsto \int_D f(\cdot, \omega) d\nu$ of the Gaussian process through the integration operator I . The standard Bayesian cubature method (c.f. Rem. 3.3) can be generalised

through the inclusion of a parametric mean function, such as used in Thm. 3.2. Due to the linearity of I , it follows that the random variable associated to this push-forward, denoted $I(f) \mid \mathcal{D}_X$, is a univariate Gaussian, whose mean and variance are now derived.

Let $k_\nu(x) = I(k(\cdot, x))$ denote the *kernel mean function* and $k_{\nu,\nu} = I(k_\nu)$ its integral. Define the row vectors p_ν and $k_{\nu,X}$ to have respective entries $[p_\nu]_j = I(p_j)$ and $[k_{\nu,X}]_j = k_\nu(x_j)$.

Theorem 3.13 (Generalised Bayesian cubature). *Consider the Gaussian process $f \mid \mathcal{D}_X$ defined in Thm. 3.2. For this process we have that $I(f) \mid \mathcal{D}_X \sim \mathcal{N}(\mu_{X,\Sigma}(f^\dagger), \sigma_{X,\Sigma}^2)$ with*

$$\mu_{X,\Sigma}(f^\dagger) = w_{k,\Sigma}^\top f_X^\dagger - w_{\pi,\Sigma}^\top \eta, \quad (18)$$

$$\sigma_{X,\Sigma}^2 = k_{\nu,\nu} + p_\nu \Sigma p_\nu^\top - (k_{\nu,X} + p_\nu \Sigma P_X^\top) w_{k,\Sigma}, \quad (19)$$

where the weight vectors $w_{k,\Sigma} \in \mathbb{R}^n$ and $w_{\pi,\Sigma} \in \mathbb{R}^Q$ are obtained from the solution of the invertible linear system

$$\begin{bmatrix} K_X & P_X \\ P_X^\top & -\Sigma^{-1} \end{bmatrix} \begin{bmatrix} w_{k,\Sigma} \\ w_{\pi,\Sigma} \end{bmatrix} = \begin{bmatrix} k_{\nu,X}^\top \\ p_\nu^\top \end{bmatrix}.$$

Equivalently, $w_{k,\Sigma} = I(u_{X,\Sigma})$ and $w_{\pi,\Sigma} = I(v_{X,\Sigma})$ for the Lagrange functions of Thm. 3.4.

Proof. From linearity of I , the random variable $I(f) \mid \mathcal{D}_X$ is Gaussian with mean and variance

$$\mu_{X,\Sigma}(f^\dagger) = \int_D s_{X,\Sigma}(f^\dagger)(x) d\nu(x), \quad (20)$$

$$\sigma_{X,\Sigma}^2 = \int_D \int_D k_{X,\Sigma}(x, x') d\nu(x) d\nu(x'). \quad (21)$$

The claim is established upon inserting the Lagrangian formulation of Thm. 3.4. □

Remark 3.14. Note that, for $\eta = 0$, the posterior mean $\mu_{X,\Sigma}(f^\dagger)$ indeed takes the form of a cubature rule, with weights $[w_{k,\Sigma}]_i$ and points $x_i \in X$.

Remark 3.15 (Bayesian cubature). As pointed out already in Rmk. 3.3, the standard Bayesian cubature method corresponds to the case $\eta = 0$ and $\Sigma = 0$ in Thm. 3.13.

3.2.2 Bayes–Sard Cubature

The Bayes–Sard cubature method is now defined as the flat prior limit (i.e. $\Sigma^{-1} \rightarrow 0$) of the generalised Bayesian cubature method:

Theorem 3.16 (Bayes–Sard cubature). *Consider the Gaussian process $f \mid \mathcal{D}_X$ defined in Thm. 3.2 and suppose that X is a π -unisolvant set. Then in the limit $\Sigma^{-1} \rightarrow 0$ we have that $I(f) \mid \mathcal{D}_X \sim \mathcal{N}(\mu_X(f^\dagger), \sigma_X^2)$ with*

$$\begin{aligned} \mu_X(f^\dagger) &= w_k^\top f_X^\dagger - w_\pi^\top \eta, \\ \sigma_X^2 &= k_{\nu,\nu} - k_{\nu,X} K_X^{-1} k_{\nu,X}^\top + (k_{\nu,X} K_X^{-1} P_X - p_\nu) w_\pi, \end{aligned} \quad (22)$$

where the weight vectors $w_k \in \mathbb{R}^n$ and $w_\pi \in \mathbb{R}^Q$ are obtained from the solution of the invertible linear system

$$\begin{bmatrix} K_X & P_X \\ P_X^\top & 0 \end{bmatrix} \begin{bmatrix} w_k \\ w_\pi \end{bmatrix} = \begin{bmatrix} k_{\nu, X}^\top \\ p_\nu^\top \end{bmatrix}. \quad (23)$$

Equivalently, $w_k = I(u_X)$ and $w_\pi = I(v_X)$ for the Lagrange functions of Thm. 3.10.

Proof. As we have only established that $s_{X, \Sigma}(f^\dagger) \rightarrow s_X(f^\dagger)$ and $k_{X, \Sigma} \rightarrow k_X$ pointwise in Thm. 3.9, we cannot directly deduce that

$$\begin{aligned} \mu_{X, \Sigma}(f^\dagger) &\rightarrow \mu_X(f^\dagger) = \int_D s_X(f^\dagger)(x) d\nu(x), \\ \sigma_{X, \Sigma}^2 &\rightarrow \sigma_X^2 = \int_D \int_D k_X(x, x') d\nu(x) d\nu(x'). \end{aligned}$$

However, that this is indeed the case can be confirmed by carrying out analysis analogous to that in the proof Thm. 3.10 for $\mu_{X, \Sigma}(f^\dagger)$ and $\sigma_{X, \Sigma}^2$ at the limit $\Sigma^{-1} \rightarrow 0$. \square

In the case where $\eta = 0$, the mean of the Bayes–Sard output takes the form of a cubature rule; i.e. $I_n(f^\dagger) = \mu_X(f^\dagger) = w_k^\top f_X^\dagger$. The *Bayes–Sard* nomenclature derives from the fact that the associated cubature rule μ_X is *exact* on the space π :

Proposition 3.17. *Assume that X is a π -unisolvent set. If $\eta = 0$, then $\mu_X(p) = p$ whenever $p \in \pi$.*

Proof. The argument is essentially identical to that of Prop. 3.11. \square

Remark 3.18. The cubature rule μ_X , for $\eta = 0$, which appears as the mean of the Bayes–Sard output, was studied in Bezhaev [1991] outside of the probabilistic context.

3.2.3 An Equivalent Kernel Perspective

In this section we aim to interpret output of the Bayes–Sard method from the perspective of the reproducing kernel. The formulation of cubature rules in reproducing kernel Hilbert spaces dates back to Larkin [1970]; Richter [1970]; Richter–Dyn [1971b,a] and Larkin [1972] and in particular the integrated kernel interpolant was studied in Bezhaev [1991] and Sommariva and Vianello [2006].

First, we recall the characterisation of Bayesian cubature rules (c.f. Rem. 3.15) as the best cubature rules in the reproducing kernel Hilbert space $H(k)$ induced by the kernel k . The *worst-case error* $e_k(X, w)$ of a cubature rule described by the points $X = \{x_1, \dots, x_n\} \subset D$ and weights $w = (w_1, \dots, w_n) \in \mathbb{R}^n$ is defined as

$$\begin{aligned} e_k(X, w) &:= \sup_{\|h\|_k \leq 1} \left| \sum_{i=1}^n w_i h(x_i) - \int_D h d\nu \right| \\ &= (k_{\nu, \nu} - 2k_{\nu, X} w + w^\top K_X w)^{1/2}. \end{aligned} \quad (24)$$

See for example [Oettershagen, 2017, Cor. 3.6] for Eqn. 24. The weights w^* of the standard Bayesian cubature rule in Rem. 3.15 are those which minimise the worst-case error among all possible weights: $w^* = \arg \min_{w \in \mathbb{R}^n} e_k(X, w)$. Conveniently, the minimum corresponds to the integration error for the kernel mean function k_ν which acts as the representer of integration (i.e., $\langle h, k_\nu \rangle_k = I(h)$ for $h \in H(k)$):

$$e_k(X, w^*) = (k_{\nu, \nu} - k_{\nu, X} w^*)^{1/2}.$$

Now, turning to Bayes–Sard cubature, from Rem. 3.12 we have that the Bayes–Sard cubature rule $\mu_X(f^\dagger)$ can be cast as an optimal cubature method based on the kernel $k_\sigma(x, x') = k(x, x') + \sigma^2 k_\pi(x, x')$ in the $\sigma \rightarrow \infty$ limit. The following therefore holds for the weights w_k and variance σ_X^2 of the Bayes–Sard cubature method:

$$w_k = \lim_{\sigma \rightarrow \infty} \arg \min_{w \in \mathbb{R}^n} e_{k_\sigma}(X, w), \quad \sigma_X^2 = \lim_{\sigma \rightarrow \infty} \min_{w \in \mathbb{R}^n} e_{k_\sigma}(X, w)^2.$$

Recall that $H(k_\sigma)$ consists of functions which can be expressed as sums of elements of $H(k)$ and π . To simplify the following argument, assume $f^\dagger \in H(k_\sigma)$. That the elements of π are exactly integrated can be clearly understood in this context. Indeed, the norm of a function $h \in H(k_\sigma)$ is [Berlinet and Thomas-Agnan, 2011, Sec. 4.1]

$$\|h\|_{k_\sigma}^2 = \min_{g \in H(k), p \in \pi} \{ \|g\|_k^2 + \sigma^2 \|p\|_{k_\pi}^2 : g + p = h \}.$$

Thus, in terms of function approximation, when $\sigma \rightarrow \infty$ the error $\|f^\dagger - h\|_{k_\sigma}$ is dominated by the error $\sigma^2 \|P_\pi(f^\dagger) - P_\pi(h)\|_{k_\pi}$ where P_π is the orthogonal projection onto π in $H(k_\sigma)$. Thus, under this norm, the approximation of $P_\pi(f^\dagger)$ in π is prioritised. In particular, when $\dim(\pi) = n$, the weights w_k are fully-determined by the requirement of exactness for functions in π and nothing is done to integrate functions in $H(k)$ well. Consequently, the limiting variance σ_X^2 must coincide with the (squared) worst-case error $e_k(X, w_k)^2$ in the RKHS $H(k)$. This final case will be considered in more detail next in the next section.

Remark 3.19. Alternatively, the limiting weights w_k can be seen as a solution to the constrained convex optimisation problem of minimising the RKHS approximation error to the kernel mean function k_ν under exactness conditions for functions in π :

$$w_k = \arg \min_{w \in \mathbb{R}^n} \|k_\nu - k_X w\|_k \quad \text{subject to} \quad P_X^\top w = p_\nu^\top.$$

This can be verified in a straightforward manner based on [DeVore et al., 2017, Section 5.2].

3.2.4 Reproduction of Classical Cubature Rules

This section presents the properties of the Bayes–Sard method in the special case where $\dim(\pi) = n$. To start, we present the following result:

Theorem 3.20. *Suppose that $\dim(\pi) = n$ and let X be a π -unisolvent set. If $\eta = 0$, then*

$$\mu_X(f^\dagger) = w_k^\top f_X^\dagger, \quad w_k^\top = p_\nu P_X^{-1}, \quad \mu_X(p) = I(p) \quad \text{for every } p \in \pi,$$

and

$$\sigma_X^2 = e_k(X, w_k)^2 = k_{\nu, \nu} - 2k_{X, \nu} w_k + w_k^\top K_X w_k.$$

That is, the Bayes–Sard cubature weights w_k are the unique weights such that every function in π is integrated exactly and the integral posterior variance σ_X^2 coincides with the worst-case error in the RKHS $H(k)$.

Proof. Due to $\dim(\pi) = n$ and X being a π -unisolvent set, the Vandermonde matrix P_X is an invertible square matrix. From Eqn. 23 we have

$$\begin{aligned} w_k &= (K_X^{-1} - K_X^{-1} P_X [P_X^\top K_X^{-1} P_X]^{-1} P_X^\top K_X^{-1}) k_{\nu, X}^\top + K_X^{-1} P_X [P_X^\top K_X^{-1} P_X]^{-1} p_\nu^\top \\ &= P_X^{-\top} p_\nu^\top. \end{aligned}$$

These are the unique weights satisfying $\sum_{j=1}^n w_{k,j} p_i(x_j) = I(p_i)$ for each basis function p_i of π . Similarly, the weights w_π take the form

$$w_\pi = [P_X^\top K_X^{-1} P_X]^{-1} P_X^\top K_X^{-1} k_{\nu, X}^\top - [P_X^\top K_X^{-1} P_X]^{-1} p_\nu^\top = P_X^{-1} k_{\nu, X}^\top - [P_X^\top K_X^{-1} P_X]^{-1} p_\nu^\top,$$

so that

$$\begin{aligned} \sigma_X^2 &= k_{\nu, \nu} - k_{\nu, X} K_X^{-1} k_{\nu, X}^\top + (P_X^\top K_X^{-1} k_{\nu, X}^\top - p_\nu^\top)^\top w_\pi \\ &= k_{\nu, \nu} - k_{\nu, X} K_X^{-1} k_{\nu, X}^\top + (P_X^\top K_X^{-1} k_{\nu, X}^\top - p_\nu^\top)^\top (P_X^{-1} k_{\nu, X}^\top - [P_X^\top K_X^{-1} P_X]^{-1} p_\nu^\top) \\ &= k_{\nu, \nu} - 2k_{\nu, X} w_k + w_k^\top K_X w_k. \end{aligned}$$

We recognise this final expression as the squared worst-case error from Eqn. 24. \square

Note that σ_X^2 only depends on π through the weights. In fact, Thm. 3.20 can be applied to *any* cubature rule, no matter how constructed: Given any distinct nodes X and non-zero weights $w \in \mathbb{R}^n$, set

$$p_i = \mathbb{1}_{D_i \setminus \{x_i\}} + \frac{\nu(D_i)}{w_i} \mathbb{1}_{\{x_i\}}$$

for disjoint sets D_i of positive measure. Under the assumption $\nu(\{x\}) = 0$ for every $x \in D$, it holds that $I(p_i) = \nu(D_i)$. The associated Vandermonde matrix is diagonal and hence can trivially be inverted. Then the Bayes–Sard method with basis $\{p_1, \dots, p_n\}$ has a posterior mean $\mu_X(f^\dagger) = w^\top f_X^\dagger$. The construction is more appealing if the weights are positive and their sum does not exceed one, since then we can use $p_i = \mathbb{1}_{D_i}$ for disjoint sets such that $\nu(D_i) = w_i$ and $x_i \in D_i$, or if the weights are naturally given by exactness conditions on π and X is π -unisolvent. Examples of such more natural constructions include uniformly weighted (quasi) Monte Carlo rules, that arise from using a partition $D = \cup_{i=1}^n D_i$ with $\nu(D_i) = 1/n$, and Gaussian tensor product rules and. This finding is summarised:

Corollary 3.21. *Suppose that $\nu(\{x\}) = 0$ for every $x \in D$. Consider a cubature rule with point set X of size n and non-zero weights $w \in \mathbb{R}^n$. Then there exists a function space π of dimension n , such that the Bayes–Sard method recovers $w_k = w$ and $\sigma_X^2 = e_k(X, w)^2$, as defined in Thm. 3.16.*

Remark 3.22 (All cubature rules are Bayes rules for some prior). If we recall that the posterior mean is a Bayes decision rule for squared-error loss [see Berger, 2013] then Cor. 3.21 demonstrates that “any cubature rule is a Bayes decision rule for some prior”; a concrete instantiation of the *complete class* theorem of Wald [1947].

Thus we have obtained a more general probabilistic interpretation of classical cubature rules than has previously been described. Indeed, in contrast to the constructions of Särkkä et al. [2016] and Karvonen and Särkkä [2017], we are able to cast $\mu_X(f^\dagger)$ as a posterior mean in such a way that the associated posterior is non-degenerate (i.e. has non-zero variance). From a practical perspective, this enables us to simultaneously achieve reliable integration performance due to, for example, polynomial exactness, *and* to perform formal uncertainty quantification for the integral based on the prior information $f^\dagger \in H(k)$.

3.3 Convergence Results

This section contains fundamental convergence results for Bayes–Sard cubature rules introduced in Sec. 3.2.2. Our attention is restricted to analysis of the cubature rule μ_X associated with the mean of the Bayes–Sard output.

3.3.1 Polynomial Basis

In this section we discuss convergence results for Bayes–Sard cubature rules in the case π is, for some $m \geq 0$, the space $\Pi_m(\mathbb{R}^d)$ of d -variate polynomials of degree at most m and $\eta = 0$. It is noteworthy that Thm. 3.24 has been derived, essentially in the form we present it, in non-probabilistic setting already by Bezhaev [1991]². For standard Bayesian cubature, the convergence results below have appeared in Briol et al. [2017] and Kanagawa et al. [2017].

When $\pi = \Pi_m(\mathbb{R}^d)$ and $\eta = 0$, the flat limit posterior mean $s_X(f^\dagger)$ defined in Eqn. 13 coincides with the interpolant defined in Wendland [2005, Section 8.5] for a conditionally positive definite kernel³. The extensive convergence theory outlined in Wendland [2005, Chapter 11] can be therefore brought to bear. We provide convergence results for the Gaussian kernel and kernels of the Matérn class that are used in the numerical experiments in Sec. 4 (however, not all our experiments are covered by Thms. 3.24 and 3.23 below); also other kernels can be handled with similar tools. For a set $X = \{x_1, \dots, x_n\} \subset D$ and D bounded, define the *fill distance*

$$h_{X,D} := \sup_{x \in D} \min_{i=1, \dots, n} \|x - x_i\|.$$

²In fact, Bezhaev [1991] appears to be the first paper to present convergence analysis for a kernel-based cubature rule.

³Note that positive definite kernels are also conditionally positive definite.

Considered as a sequence of sets indexed by $n \in \mathbb{N}$, we say that X is *quasi-uniform* in D if $h_{X,D} \lesssim n^{-1/d}$.

Theorem 3.23 (Spectral convergence for Gaussian kernels). *Let D be a hypercube in \mathbb{R}^d , $\eta = 0$, and let X be a $\Pi_m(\mathbb{R}^d)$ -unisolvent set for some $m \geq 0$. Consider the Gaussian kernel*

$$k(x, x') = \exp\left(-\frac{\|x - x'\|^2}{2\ell^2}\right) \quad (25)$$

for a length-scale $\ell > 0$. Then there is $c > 0$ such that, for $h_{X,D}$ sufficiently small, the estimate

$$|\mu_X(f^\dagger) - I(f^\dagger)| \leq e^{-c/h_{X,D}^{1-\varepsilon}} \|f^\dagger\|_k$$

holds for any $\varepsilon > 0$. In particular, for a quasi-uniform point set we have the estimate

$$|\mu_X(f^\dagger) - I(f^\dagger)| \lesssim e^{-cn^{1/d-\varepsilon}} \|f^\dagger\|_k$$

for any $\varepsilon > 0$.

Proof. By Wendland [Theorem 11.22 of 2005], there is $c > 0$ such that

$$\sup_{x \in D} |s_X(f^\dagger)(x) - f^\dagger(x)| \leq e^{c \log(h_{X,D})/h_{X,D}} \|f^\dagger\|_k.$$

for a sufficiently small $h_{X,D}$. Thus

$$|\mu_X(f^\dagger) - I(f^\dagger)| = |I(s_X(f^\dagger) - f^\dagger)| \leq I(|s_X(f^\dagger) - f^\dagger|) \leq e^{c \log(h_{X,D})/h_{X,D}} \|f^\dagger\|_k$$

because the Bayes–Sard cubature rule $\mu_X(f^\dagger)$ is the integral of $s_X(f^\dagger)$ and ν is a probability measure. Since $\log(h_{X,D})/h_{X,D} \leq -1/h_{X,D}^{1-\varepsilon}$ for any $\varepsilon > 0$ when $h_{X,D}$ is small enough, we obtain the required result. \square

The next result extends [Kanagawa et al., 2017, Proposition 4] for the standard Bayesian cubature method. Its proof follows that of Thm. 3.23 and is an application of Wendland [Corollary 11.33 in 2005].

Theorem 3.24 (Polynomial convergence for Sobolev kernels). *Let $\eta = 0$ and X be a $\Pi_m(\mathbb{R}^d)$ -unisolvent set for some $m \geq 0$. Suppose that*

- (i) D is a bounded open set that satisfies an interior cone condition and whose boundary ∂D is Lipschitz;
- (ii) for $\alpha > d/2$, the RKHS of the kernel k is norm-equivalent to the Sobolev space $H^\alpha(D)$. (i.e. there exists a finite constant $0 < c < \infty$ such that $c^{-1}\|f\|_k \leq \|f\|_{H^\alpha(D)} \leq c\|f\|_k$.)
- (iii) the density function of ν is bounded.

Then the estimate

$$|\mu_X(f^\dagger) - I(f^\dagger)| \lesssim h_{X,D}^\alpha \|f^\dagger\|_{H^\alpha(D)}$$

holds. In particular, for a quasi-uniform point set

$$|\mu_X(f^\dagger) - I(f^\dagger)| \lesssim n^{-\alpha/d} \|f^\dagger\|_{H^\alpha(D)}.$$

Remark 3.25. The Matérn kernel

$$k(x, x') = \frac{2^{1-\rho}}{\Gamma(\rho)} \left(\frac{\sqrt{2\rho} \|x - x'\|}{\ell} \right)^\rho K_\rho \left(\frac{\sqrt{2\rho} \|x - x'\|}{\ell} \right), \quad (26)$$

where Γ is the gamma function and K_ρ the modified Bessel function of the second kind, with positive parameters ρ and ℓ , satisfies Assumption (ii) of the above theorem with $\alpha = \rho + \frac{d}{2}$.

3.3.2 Reproduced Classical Cubature Rules

As pointed out in Cor. 3.21, the mean $\mu_X(f^\dagger)$ of the Bayes–Sard output can be arranged to coincide with any given cubature rule through judicious choice of the function space π , provided that its dimension matches the number of nodes x_i that are used. In this case, convergence rates are trivially inherited. For example, and for simplicity letting ν be uniform on $D = [0, 1]^d$,

- nodes drawn randomly (or through utilisation of a Markov Chain) from ν and uniform weights yield the standard (probabilistic) Monte Carlo rate

$$\mathbb{E}(|\mu_X^{\text{MC}}(f^\dagger) - I(f^\dagger)|^2)^{\frac{1}{2}} \lesssim n^{-1/2} \|f^\dagger\|_{L^2(D)};$$

- certain quasi-Monte Carlo nodes and uniform weights can attain polynomial rates

$$|\mu_X^{\text{QMC}}(f^\dagger) - I(f^\dagger)| \lesssim n^{-\alpha} \|f^\dagger\|_{H_{\text{mix}}^\alpha(D)}$$

for $\alpha \geq 2$ and functions with dominating mixed smoothness. See [Dick and Pillichshammer, 2010, Chapter 15] for these results and for the formal definition of the norm;

- certain sparse grid methods on hypercubes have the rates

$$\begin{aligned} |\mu_X^{\text{SG}}(f^\dagger) - I(f^\dagger)| &\lesssim n^{-\alpha/d} (\log n)^{(d-1)(\alpha/d+1)} \|f^\dagger\|_{C^\alpha(D)}, \\ |\mu_X^{\text{SG}}(f^\dagger) - I(f^\dagger)| &\lesssim n^{-\alpha} (\log n)^{(d-1)(\alpha+1)} \|f^\dagger\|_{F^\alpha(D)} \end{aligned}$$

for functions having bounded derivatives or bounded mixed derivatives up to order α , respectively. See [Novak and Ritter, 1996, 1997, 1999] for these results and for formal definitions of the norms.

This completes our preliminary convergence analysis for the Bayes–Sard method. The impact of the choice of finite-dimensional space π will be assessed in more detail in subsequent work.

4 Experimental Results

This section presents a trio of numerical experiments designed to investigate the empirical performance of the Bayes–Sard cubature method:

- Examples in Secs. 4.2 and 4.3 consider the case when π is a polynomial space such that $\dim(\pi) < n$. The examples demonstrate that the Bayes–Sard cubature is typically at least as accurate as standard Bayesian cubature whilst being less sensitive to misspecification of the length-scale parameter in the kernel.
- In Sec. 4.4 we consider the case $\dim(\pi) = n$, described in Sec. 3.2.4, when the cubature weights are independent of selection of the kernel. The example shows that the Bayes–Sard method is capable of providing consistent uncertainty quantification for a classical numerical integration method based on polynomial exactness.

Recall from Thms. 3.9 and 3.16 that considerations involving the limit $\Sigma^{-1} \rightarrow 0$ entail assuming that the point set X is π -unisolvent. In the example of Sec. 4.2 this causes no issues as the domain is one-dimensional. However, the example of Sec. 4.3 involves randomly drawn point sets in higher dimensions. This is not a problem in practice since having all points confined to a hyperplane ($\pi = \Pi_1(\mathbb{R}^d)$ is used in this example) is a measure zero event. Throughout we fixed $\eta = 0$, which is a natural default.

4.1 On Choosing the Kernel Parameters

The stationary kernels typically used in Gaussian process regression are parametrised by positive *length-scale*⁴ and *amplitude* parameters ℓ and λ , respectively:

$$k(x, x') = k(x - x') = \lambda k_0((x - x')/\ell)$$

for, in a slight abuse of notation, some base kernel k_0 . Adapting these parameters in a data-dependent way is an essential prerequisite for meaningful quantification of uncertainty for the integral. For the experiments below we set these parameters independently, following the approach used in Briol et al. [2017, Sec. 4.1].

4.1.1 Amplitude Parameter

If the amplitude parameter is given the improper prior $p(\lambda) \propto 1/\lambda$, then the posterior marginal at the flat prior limit $\Sigma^{-1} \rightarrow 0$ for $I(f)$ is Student- t with the mean $\mu_X(f^\dagger)$ and variance $((f_X^\dagger)^\top K_X^{-1} f_X^\dagger / n) \sigma_X^2$. That is, the Bayes–Sard variance, as given in Thm. 3.16 or 3.20, gets scaled by a data-dependent constant.

⁴In general, a distinct length scale parameter for each dimension could be used.

4.1.2 Length-Scale Parameter

The length-scale ℓ is typically more challenging to adapt and in what follows we used the *empirical Bayes* method. This involves maximisation of the log-marginal likelihood of the regression model in Thm. 3.9 [Rasmussen and Williams, 2006, Eqns. 2.29 and 2.45]:

$$\begin{aligned}
 & -\frac{1}{2}(f_X^\dagger)^\top K_{\ell,X}^{-1} f_X^\dagger + \frac{1}{2}(f_X^\dagger)^\top K_{\ell,X}^{-1} P_X [P_X^\top K_{\ell,X}^{-1} P_X]^{-1} P_X^\top K_{\ell,X}^{-1} f_X^\dagger \\
 & - \frac{1}{2} \log \det(K_{\ell,X}) - \frac{1}{2} \log \det(P_X^\top K_{\ell,X}^{-1} P_X) - \frac{n - \dim(\pi)}{2} \log(2\pi),
 \end{aligned} \tag{27}$$

where the additional subscript for the kernel matrix signifies that this matrix is dependent on the length-scale parameter.

In the case where $\dim(\pi) = n$ and P_X is an invertible square matrix, the first two data-dependent terms in Eqn. (27) cancel. This is undesirable from the perspective of uncertainty quantification, as the length scale parameter is no longer data-dependent. In this case, we therefore suggest proceeding pragmatically and using the log-marginal likelihood associated with a standard Gaussian process model:

$$-\frac{1}{2}(f_X^\dagger)^\top K_{\ell,X}^{-1} f_X^\dagger - \frac{1}{2} \log \det(K_{\ell,X}) - \frac{n}{2} \log(2\pi). \tag{28}$$

Recall that, in the $\dim(\pi) = n$ case, the choice of the kernel and its parameters only affects uncertainty quantification for the integral; the mean of the Bayes–Sard method is still guaranteed to coincide with the selected classical cubature method.

Note that the examples in Secs. 4.2 and 4.3 for the $\dim(\pi) < n$ case are concerned with sensitivity of Bayes–Sard integral estimates to misspecified length-scale rather than fitting of the length-scale based on Eqn. (27). Dependence on the length-scale could be also included in the basis $\{p_1, \dots, p_Q\}$ for π by selecting, for example, $p_i(x) = p_{0,i}(x/\ell)$ for some fixed functions $\{p_{0,1}, \dots, p_{0,Q}\}$. However, this was not pursued in the examples.

4.2 A One-Dimensional Toy Example

Our first example is one-dimensional. The test function that we considered was

$$f^\dagger(x) = \exp\left(\sin(2x) - \frac{x^2}{5}\right) + \frac{x^2}{2}$$

and the measure ν was the standard normal. The effect the length-scale ℓ of the Gaussian kernel (25) has on the performance of the standard Bayesian quadrature and the Bayes–Sard quadrature of Sec. 3.2, with $\pi = \Pi_m(\mathbb{R})$ for different m , was investigated. The true integral in this benchmark is

$$I(f^\dagger) = \frac{1}{\sqrt{2\pi}} \int_{\mathbb{R}} f^\dagger(x) e^{-x^2/2} dx \approx 2.0693. \tag{29}$$

Results for three different values for the polynomial degree m and the number of nodes n are depicted in Fig. 2. It can be observed that the Bayes–Sard quadrature is more robust

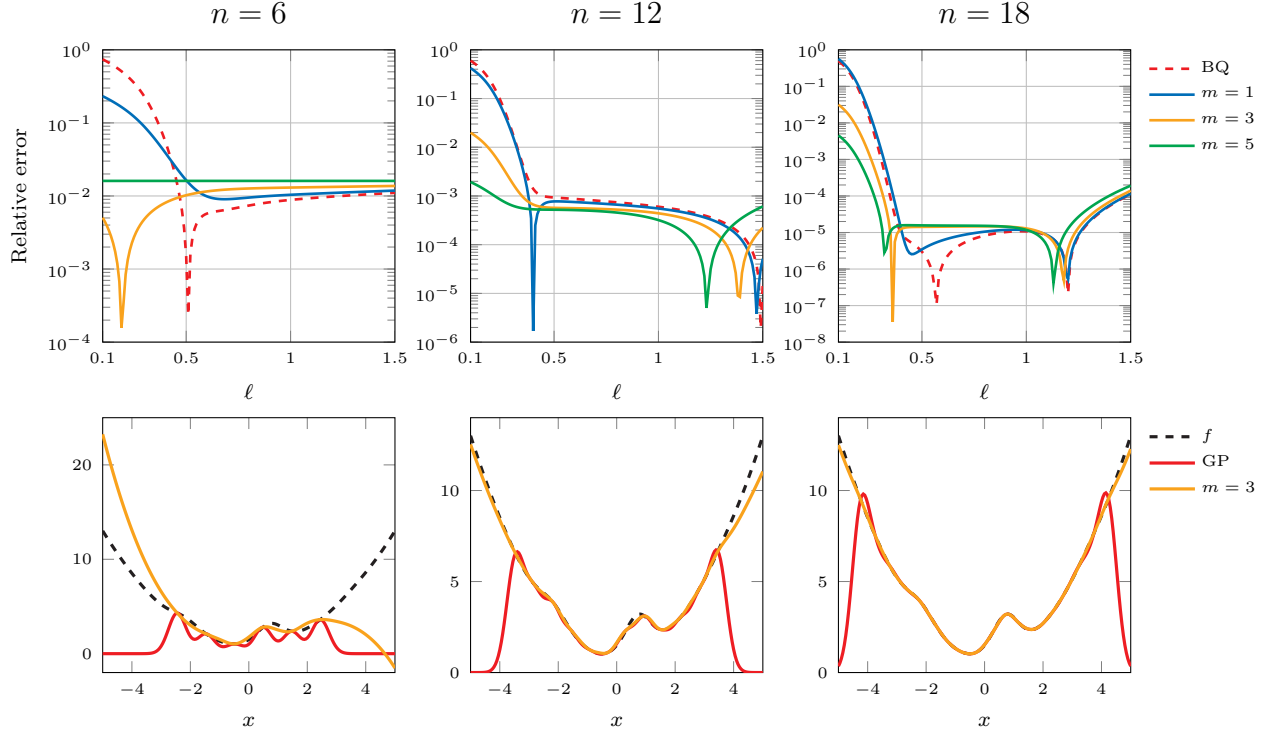


Figure 2: Approximation of the Gaussian integral (29) using Bayesian quadrature (BQ) and Bayes-Sard quadrature with $\pi = \Pi_m(\mathbb{R})$ ($m = 1, 3, 5$), both based on the Gaussian kernel with varying length-scale parameter ℓ . The n nodes have been placed uniformly on the interval $[-\sqrt{n}, \sqrt{n}]$ for $n = 6, 12, 18$. The upper row presents the relative integration error $|I(f^\dagger) - I_n(f^\dagger)|/I(f^\dagger)$ for each quadrature rule I_n as a function of the length-scale. The lower row contains the corresponding posterior means for $\ell = 0.3$, a value too small. The “optimal” length-scales ℓ^* for BQ, as computed by maximising the standard GP log-likelihood (28), are $\ell^* = 0.7851$, $\ell^* = 0.6698$, and $\ell^* = 0.6451$ for $n = 6$, $n = 12$, and $n = 18$, respectively. That the Bayes-Sard rule for $m = 5$ and $n = 6$ is ℓ -independent is due to exact reproduction of a purely polynomial method since there is a unique polynomial interpolant of degree 5 to the data (recall Sec. 3.2.4).

compared to Bayesian quadrature when the length-scale is misspecified, particularly when there are only a few nodes. This is because the polynomial part mitigates the tendency of the posterior mean to revert quickly back to zero. For reasonable values of the length-scale, the accuracy of the different methods is comparable.

4.3 Zero Coupon Bonds

This section experiments with the high-dimensional zero coupon bonds example that has been used previously in numerical experiments for kernel cubature by Karvonen and Särkkä [2018a, Sec. 5.5]. See Holtz [2011, Sec. 6.1] for more details on this example. The d -step Euler-Maruyama with uniform step-size $\Delta t = T/D$ of the Vasicek model

$$dr(t) = \kappa(\theta - r(t))dt + \sigma dW(t),$$

where $W(t)$ is the standard Brownian motion and κ , θ , and σ are positive parameters, is

$$r_{t_i} = r_{t_{i-1}} + \kappa(\theta - r_{t_{i-1}})\Delta t + \sigma\sqrt{\Delta t}x_{t_i}, \quad i = 1, \dots, d,$$

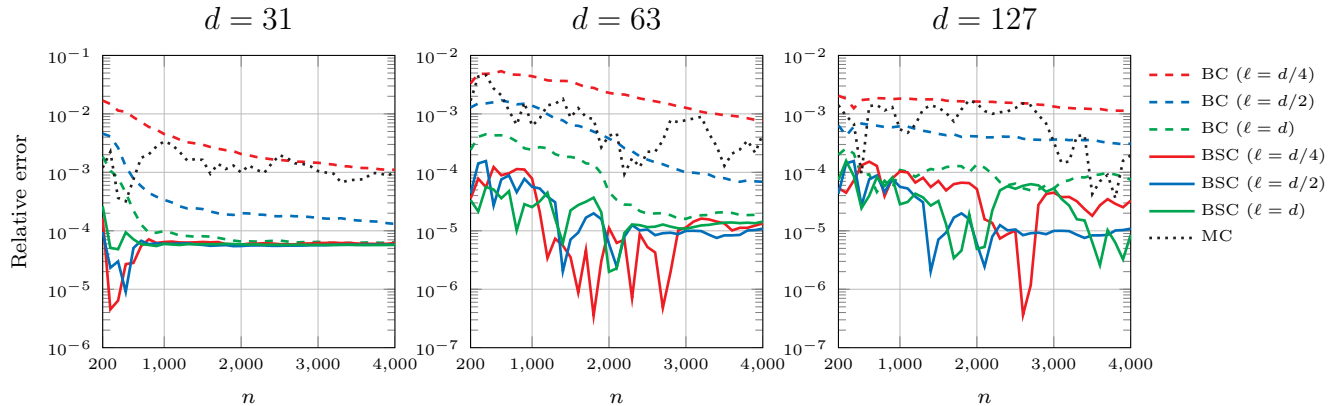


Figure 3: Approximation of the d -dimensional Gaussian expectation (30) using Bayesian cubature (BC) and Bayes–Sard cubature (BSC) with $\pi = \Pi_1(\mathbb{R}^d)$, both based on the Gaussian kernel with different length-scales ℓ . Each figure contains relative errors $|I(f^\dagger) - I_n(f^\dagger)|/I(f^\dagger)$ for each cubature rule I_n , for a given dimension and three different length-scales as a function of the number of nodes n that have been drawn randomly from the standard Gaussian distribution. The standard Monte Carlo approximation (MC) is also plotted for comparison.

for independent standard Gaussian random variables x_{t_i} and some initial value r_{t_0} . The quantity of interest is the Gaussian expectation

$$P(0, T) := \mathbb{E} \left[\exp \left(- \Delta t \sum_{i=0}^{D-1} r_{t_i} \right) \right] = \exp(-\Delta t r_{t_0}) \mathbb{E} \left[\exp \left(- \Delta t \sum_{i=1}^{D-1} r_{t_i} \right) \right] \quad (30)$$

of dimension $d := D - 1$. This expectation admits the closed-form solution

$$P(0, T) = \exp \left(- \frac{(\gamma + \beta_D r_{t_0}) T}{d} \right)$$

for certain constants γ and β_D . We use the same parameter values as in the aforementioned references and compare accuracy of standard Bayesian cubature to Bayes–Sard cubature with $\pi = \Pi_1(\mathbb{R}^d)$ with different dimensions d and length-scales ℓ of the Gaussian kernel. In Karvonen and Särkkä [2018a, Sec. 5.5] it was observed that $\ell \approx d$ results in accurate estimates by the Bayesian cubature for this integration problem. As in Sec. 4.2, it is apparent from Fig. 3 that the Bayes–Sard cubature is less sensitive to misspecification of the length-scale parameter compared to the standard Bayesian cubature method. This is again due to the improved extrapolation performance conferred through the polynomial component.

4.4 Clenshaw–Curtis Quadrature

This final example explores the case $\dim(\pi) = n$ that, as discussed in Sec. 3.2.4, enables any cubature rule to be endowed with a probabilistic output through judicious selection of π , the variance of which is controlled by choice of the kernel. It is demonstrated that the uncertainty quantification provided by the Bayes–Sard method for the integral can be meaningful.

The example is concerned with classical Clenshaw–Curtis quadrature rules [Clenshaw and Curtis, 1960; Trefethen, 2008] on the interval $D = [-1, 1]$ with the uniform probability

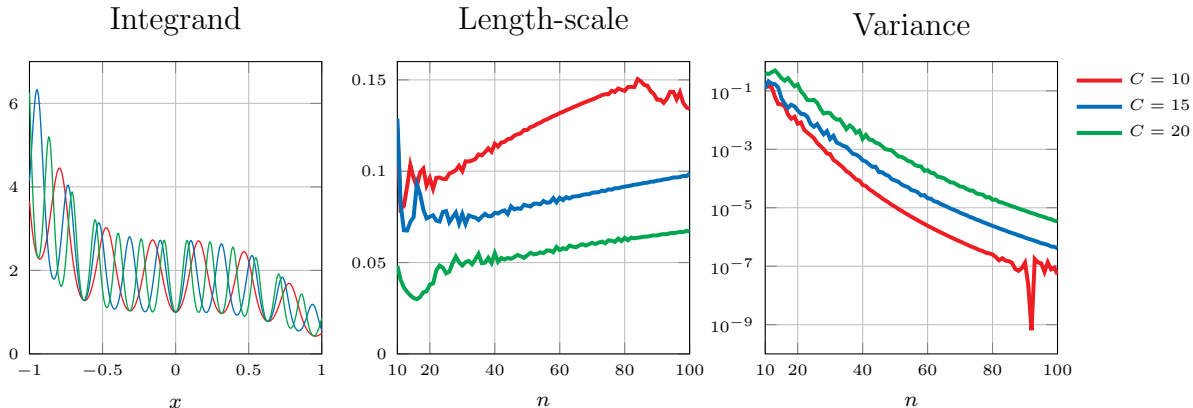


Figure 4: Uncertainty quantification by the Bayes–Sard method using the Matérn kernel (32) for the n -point Clenshaw–Curtis quadrature approximation to the integral $\frac{1}{2} \int_{-1}^1 f^\dagger(x) dx$ of the function (31) with $C \in \{10, 15, 20\}$. We have, from left to right: (i) integrand functions; (ii) length-scales of the Matérn kernel as computed by empirical Bayes using the GP log-likelihood (28) and (iii) posterior marginal Bayes–Sard variances. Note that the Clenshaw–Curtis point sets used here are not in general nested.

measure $d\nu(x) = \frac{1}{2} dx$. Attractiveness of these polynomial quadrature rules stems from the facts that their nodes and weights can be efficiently computed by the means of fast Fourier transform and that the point sets are nested for $n = 2^m + 1$, $m \geq 0$.

The test function

$$f^\dagger(x) = \exp(\sin(Cx)^2 - x^3) \quad (31)$$

was considered with $C \in \{10, 15, 20\}$ and (somewhat arbitrarily) the Matérn kernel (26) with $\rho = 5/2$ and the length-scale amplitude parameters ℓ and λ :

$$k(x, x') = \lambda \left(1 + \frac{\sqrt{5}|x - x'|}{\ell} + \frac{5|x - x'|^2}{3\ell^2} \right) \exp\left(-\frac{\sqrt{5}|x - x'|}{\ell} \right). \quad (32)$$

The kernel mean function k_ν and its integral $k_{\nu,\nu}$ are available in closed form for this kernel. For meaningful uncertainty quantification it is imperative that the posterior variance of $I(f)$ is made data-dependent by tuning the kernel parameters ℓ and λ , and this was achieved as outlined in Sec. 4.1.

The results of this experiment are depicted in Fig. 4. We observe that behaviour of both the length-scales and posterior integral variances is as one would expect: for larger C , which corresponds to a more oscillating and challenging integrand, the estimated length-scale is smaller and there is more uncertainty expressed in the Bayes–Sard output.

5 Discussion

This paper proposed a Bayes–Sard cubature method, which provides an explicit connection between classical cubatures and the Bayesian inferential framework. In particular, we obtained polynomially exact generalisations of the standard Bayesian cubature method in Thm. 3.16 and demonstrated in Cor. 3.21 how any classical cubature rule can be recovered as the output

of a probabilistic model such that its variance coincides with the classical worst-case error of the rule in a reproducing kernel Hilbert space.

The main practical consideration with Bayesian and Bayes–Sard cubature is selection of the kernel. The point estimator associated to the standard Bayesian cubature method is wholly driven by the kernel and its parameters, in particular the length-scale, rendering the method virtually useless if these cannot be properly elicited or learned. The data-driven estimation of kernel parameters can require that the number n of data exceeds several thousands, at which point the cubic cost associated with the method becomes impractical. In contrast, as demonstrated in Sec. 4, the point estimator associated to the Bayes–Sard output inherits reliable performance that is relatively independent of the kernel. This robust performance is in line with many non-probabilistic methods of numerical integration, and should serve to widen the appeal of Bayesian methods in that context. In addition, we believe that approximate fast Gaussian process methods, such as those appearing in Hensman et al. [2018] and Zhou et al. [2018], could be used for efficient automatic selection of kernel parameters with little adverse effect on accuracy of the point estimator in the Bayes–Sard method.

On the other hand, further work is yet required to assess the quality of the uncertainty quantification provided by the Bayes–Sard method. This will require careful analysis that accounts for how kernel parameters are estimated, and is expected to be technically more challenging [see, e.g., Xu and Stein, 2017].

Acknowledgements The authors are grateful for discussion with Aretha Teckentrup and Catherine Powell. TK was supported by the Aalto ELEC Doctoral School. CJO was supported by the Lloyd’s Register Foundation programme on data-centric engineering. This material was based upon work partially supported by the National Science Foundation under Grant DMS-1127914 to the Statistical and Applied Mathematical Sciences Institute. Any opinions, findings, and conclusions or recommendations expressed in this material are those of the author(s) and do not necessarily reflect the views of the National Science Foundation.

References

- Ba, B. S. and Joseph, R. (2012). Composite Gaussian process models for emulating expensive functions. *The Annals of Applied Statistics*, 6(4):1838–1860.
- Bach, F. (2017). On the equivalence between kernel quadrature rules and random feature expansions. *Journal of Machine Learning Research*, 18(21):1–38.
- Berger, J. (2013). *Statistical Decision Theory: Foundations, Concepts, and Methods*. Springer Science & Business Media.
- Berlinet, A. and Thomas-Agnan, C. (2011). *Reproducing Kernel Hilbert Spaces in Probability and Statistics*. Springer Science & Business Media.

- Bezhaev, A. Yu. (1991). Cubature formulae on scattered meshes. *Soviet Journal of Numerical Analysis and Mathematical Modelling*, 6(2):95–106.
- Bogachev, V. I. (1998). *Gaussian Measures*. Number 62 in Mathematical Surveys and Monographs. American Mathematical Society.
- Briol, F.-X., Oates, C. J., Girolami, M., Osborne, M. A., and Sejdinovic, D. (2017). Probabilistic integration: A role in statistical computation? *arXiv:1512.00933v6*.
- Caliari, M., De Marchi, S., and Vianello, M. (2005). Bivariate polynomial interpolation on the square at new nodal sets. *Applied Mathematics and Computation*, 165(2):261–274.
- Chai, H. and Garnett, R. (2018). An improved Bayesian framework for quadrature of constrained integrands. *arXiv:1802.04782*.
- Clenshaw, C. W. and Curtis, A. R. (1960). A method for numerical integration on an automatic computer. *Numerische Mathematik*, 2(1):197–205.
- Cockayne, J., Oates, C. J., Sullivan, T., and Girolami, M. (2017). Bayesian probabilistic numerical methods. *arXiv:1702.03673v2*.
- Davis, P. J. and Rabinowitz, P. (2007). *Methods of Numerical Integration*. Courier Corporation.
- DeVore, R., Foucart, S., Petrova, G., and Wojtaszczyk, P. (2017). Computing a quantity of interest from observational data. *Preprint*. http://www.math.tamu.edu/~foucart/publi/DFPW_recovery_v12.pdf.
- Diaconis, P. (1988). Bayesian numerical analysis. In *Statistical Decision Theory and Related Topics IV*, volume 1, pages 163–175. Springer-Verlag New York.
- Dick, J. and Pillichshammer, F. (2010). *Digital Nets and Sequences: Discrepancy Theory and Quasi-Monte Carlo Integration*. Cambridge University Press.
- Driscoll, T. A. and Fornberg, B. (2002). Interpolation in the limit of increasingly flat radial basis functions. *Computers & Mathematics with Applications*, 43(3–5):413–422.
- Fasshauer, G. E. (2007). *Meshfree Approximation Methods with MATLAB*. Number 6 in Interdisciplinary Mathematical Sciences. World Scientific.
- Gautschi, W. (2004). *Orthogonal Polynomials: Computation and Approximation*. Numerical Mathematics and Scientific Computation. Oxford University Press.
- Gunter, T., Osborne, M. A., Garnett, R., Hennig, P., and Roberts, S. J. (2014). Sampling for inference in probabilistic models with fast Bayesian quadrature. In *Advances in Neural Information Processing Systems*, pages 2789–2797.

- Gunzburger, M. and Teckentrup, A. L. (2014). Optimal point sets for total degree polynomial interpolation in moderate dimensions. *arXiv:1407.3291*.
- Hennig, P., Osborne, M. A., and Girolami, M. (2015). Probabilistic numerics and uncertainty in computations. *Proceedings of the Royal Society of London A: Mathematical, Physical and Engineering Sciences*, 471(2179).
- Hensman, J., Durrande, N., and Solin, A. (2018). Variational fourier features for Gaussian processes. *Journal of Machine Learning Research*. Accepted for publication.
- Hickernell, F. (1998). A generalized discrepancy and quadrature error bound. *Mathematics of Computation*, 67(221):299–322.
- Holtz, M. (2011). *Sparse Grid Quadrature in High Dimensions with Applications in Finance and Insurance*. Number 77 in Lecture Notes in Computational Science and Engineering. Springer.
- Kanagawa, M., Sriperumbudur, B. K., and Fukumizu, K. (2016). Convergence guarantees for kernel-based quadrature rules in misspecified settings. In *Advances in Neural Information Processing Systems*, pages 3288–3296.
- Kanagawa, M., Sriperumbudur, B. K., and Fukumizu, K. (2017). Convergence analysis of deterministic kernel-based quadrature rules in misspecified settings. *arXiv:1709.00147*.
- Karlin, S. and Studden, W. J. (1966). *Tchebycheff Systems: With Applications in Analysis and Statistics*. Interscience Publishers.
- Karvonen, T. and Särkkä, S. (2017). Classical quadrature rules via Gaussian processes. In *27th IEEE International Workshop on Machine Learning for Signal Processing*.
- Karvonen, T. and Särkkä, S. (2018a). Fully symmetric kernel quadrature. *SIAM Journal on Scientific Computing*, 40(2):A697–A720.
- Karvonen, T. and Särkkä, S. (2018b). Gaussian kernel quadrature at scaled Gauss–Hermite nodes. *arXiv:1803.09532*.
- Kennedy, M. C. and O’Hagan, A. (2001). Bayesian calibration of computer models. *Journal of the Royal Statistical Society: Series B (Statistical Methodology)*, 63(3):425–464.
- Larkin, F. (1972). Gaussian measure in Hilbert space and applications in numerical analysis. *The Rocky Mountain Journal of Mathematics*, 2(3):379–421.
- Larkin, F. M. (1970). Optimal approximation in Hilbert spaces with reproducing kernel functions. *Mathematics of Computation*, 24(112):911–921.
- Lee, Y. J., Yoon, G. J., and Yoon, J. (2007). Convergence of increasingly flat radial basis interpolants to polynomial interpolants. *SIAM Journal on Mathematical Analysis*, 39(2):537–553.

- Minka, T. (2000). Deriving quadrature rules from Gaussian processes. Technical report, Statistics Department, Carnegie Mellon University.
- Novak, E. and Ritter, K. (1996). High dimensional integration of smooth functions over cubes. *Numerische Mathematik*, 75(1):79–97.
- Novak, E. and Ritter, K. (1997). The curse of dimension and a universal method for numerical integration. In *Multivariate Approximation and Splines*, pages 177–187. Birkhäuser Basel.
- Novak, E. and Ritter, K. (1999). Simple cubature formulas with high polynomial exactness. *Constructive Approximation*, 15(4):499–522.
- Oates, C. J., Niederer, S., Lee, A., Briol, F.-X., and Girolami, M. (2017). Probabilistic models for integration error in the assessment of functional cardiac models. In *Advances in Neural Information Processing Systems*, pages 109–117.
- Oetersshagen, J. (2017). *Construction of Optimal Cubature Algorithms with Applications to Econometrics and Uncertainty Quantification*. PhD thesis, Institut für Numerische Simulation, Universität Bonn.
- O’Hagan, A. (1978). Curve fitting and optimal design for prediction. *Journal of the Royal Statistical Society. Series B (Methodological)*, 40(1):1–42.
- O’Hagan, A. (1991). Bayes–Hermite quadrature. *Journal of Statistical Planning and Inference*, 29(3):245–260.
- O’Hagan, A. (1992). Some Bayesian numerical analysis. *Bayesian Statistics*, 4:345–363.
- Osborne, M., Garnett, R., Ghahramani, Z., Duvenaud, D. K., Roberts, S. J., and Rasmussen, C. E. (2012a). Active learning of model evidence using Bayesian quadrature. In *Advances in Neural Information Processing Systems*, pages 46–54.
- Osborne, M., Garnett, R., Roberts, S., Hart, C., Aigrain, S., and Gibson, N. (2012b). Bayesian quadrature for ratios. In *Artificial Intelligence and Statistics*, pages 832–840.
- Owhadi, H. and Scovel, C. (2015). Conditioning Gaussian measure on Hilbert space. *arXiv:1506.04208*.
- Rasmussen, C. E. and Williams, C. K. (2006). *Gaussian Processes for Machine Learning*. MIT Press.
- Richter, N. (1970). Properties of minimal integration rules. *SIAM Journal on Numerical Analysis*, 7(1):67–79.
- Richter-Dyn, N. (1971a). Minimal interpolation and approximation in Hilbert spaces. *SIAM Journal on Numerical Analysis*, 8(3):583–597.

- Richter-Dyn, N. (1971b). Properties of minimal integration rules. II. *SIAM Journal on Numerical Analysis*, 8(3):497–508.
- Sard, A. (1949). Best approximate integration formulas; best approximation formulas. *American Journal of Mathematics*, 71(1):80–91.
- Särkkä, S., Hartikainen, J., Svensson, L., and Sandblom, F. (2016). On the relation between Gaussian process quadratures and sigma-point methods. *Journal of Advances in Information Fusion*, 11(1):31–46.
- Sauer, T. and Xu, Y. (1995). On multivariate Lagrange interpolation. *Mathematics of Computation*, 64(211):1147–1170.
- Schaback, R. (2005). Multivariate interpolation by polynomials and radial basis functions. *Constructive Approximation*, 21(3):293–317.
- Schober, M., Duvenaud, D., and Hennig, P. (2014). Probabilistic ODE solvers with Runge-Kutta means. In *Advances in Neural Information Processing Systems*, volume 27, pages 739–747.
- Schoenberg, I. J. (1964). Spline interpolation and best quadrature formulae. *Bulletin of the American Mathematical Society*, 70(1):143–148.
- Sommariva, A. and Vianello, M. (2006). Numerical cubature on scattered data by radial basis functions. *Computing*, 76(3–4):295–310.
- Teymur, O., Zygalakis, K., and Calderhead, B. (2016). Probabilistic linear multistep methods. In *Advances in Neural Information Processing Systems*, volume 29, pages 4321–4328.
- Trefethen, L. N. (2008). Is Gauss quadrature better than Clenshaw–Curtis? *SIAM Review*, 50(1):67–87.
- Wald, A. (1947). An essentially complete class of admissible decision functions. *The Annals of Mathematical Statistics*, pages 549–555.
- Wendland, H. (2005). *Scattered Data Approximation*, volume 28 of *Cambridge Monographs on Applied and Computational Mathematics*. Cambridge University Press.
- Xu, W. and Stein, M. (2017). Maximum likelihood estimation for a smooth Gaussian random field model. *SIAM/ASA Journal on Uncertainty Quantification*, 5(1):138–175.
- Zhou, Q., Liu, W., Li, J., and Marzouk, Y. M. (2018). An approximate empirical Bayesian method for large-scale linear-Gaussian inverse problems. *arXiv:1705.07646v2*.